DOI: 10.21062/mft.2026.002 http://www.journalmt.com

Control Measurement of Car Tires during Transport on a Conveyor

Patrik Balcar (0009-0007-4924-5681)[1], Pavel Houška (0000-0003-4295-258X)[1], Martin Svoboda (0000-0002-7344-1531)[1], Ondřej Vetchý[1], Milan Chalupa (0000-0002-9366-1371)[2], Milan Sapieta (0000-0003-1356-1168)[3], Roman Horký (0000-0002-4451-3006)[1]

[1]Faculty of Mechanical Engineering, Jan Evangelista Purkyně University in Ústí nad Labem. Pasteurova 3334/7, 400 01 Ústí nad Labem, Czech Republic, pavel.houska@ujep.cz, patrik.balcar@ujep.cz,martin.svoboda@ujep.cz, ondrej.vetchky@ujep.cz, roman.horky@ujep.cz

[2]Faculty of Military Technology, University of Defence in Brno, Czech Republic, milan.chalupa@unob.cz

[3]Faculty of Mechanical Engineering, Univerzity of Zilina. Univerzitna 1, 010 26 Zilina. Slovak Republic. E-mail: milan.sapieta@fstroj.uniza.sk

The aim of this work is to verify the reliability of optical inspection of tires during their transport on a roller conveyor, with an emphasis on the accuracy of 3D scanning in real and simulated operating conditions. A measuring box was designed and constructed to eliminate environmental interference, and measurements were subsequently compared with different degrees of site coverage. Testing was carried out using a 3D sensor O3D302 operating on the Time-of-Flight principle, and spatial data in the form of point clouds were obtained and compared with the reference dimensions of the Nokian WR D4 tire. The effects of solar IR radiation, rain, surface moisture, and natural lighting conditions were analyzed, which caused different levels of deformation, noise, and measurement deviations. The results show that significant errors occur without coverage, while the measuring box significantly reduces these deviations and increases the stability of point data. Complete coverage from above and below proved to be the most effective solution, but the wet tire surface remains a significant source of interference. The work further proposes structural modifications to the box and recommends the application of a matte surface and the expansion of tests to include the effects of vibrations and real conveyor operation. The result is a technical evaluation of the measurements and recommendations for improving optical tire detection in the industrial process.

Keywords: Experiment, Measurement, Roller Conveyor, Reliability, Pneumatics

1 Introduction

Currently, the issue of waste management is one of the key topics in the field of environmental protection. Conveyors play a significant role in industrial logistics and production processes. They enable the efficient transport of materials and products, thereby contributing to the optimization of production and reduction of operating costs.

Modern technologies allow the integration of various measuring and control systems that ensure the accuracy and reliability of handling of transported objects. This makes it possible to streamline the sorting, quality control and subsequent processing of materials in various industrial sectors.

A significant source of waste is used tires, which, if not processed correctly, represent a significant environmental burden. Tires are often transported to cement plants, power plants and other facilities, where they are further processed and burned as an alternative fuel. However, this process requires inspection and control of tires to ensure their trouble-free transport.

The field of 3D scanning has been developing dynamically in recent years and is finding increasingly widespread application in various industrial sectors. This technology enables detailed scanning and digitization of object surfaces, which is useful not only in the field of quality control, but also in the field of automation and optimization of production processes.

Contact 3D scanners operate on the principle of direct physical contact with the surface of the scanned object. These scanners use a movable probe with a sensitive sensor that monitors the change in position on the surface of the object, while measuring its dimensions. Usually, these are devices that are capable of measuring only small objects, while the scanner requires fixation of the examined object on a special surface to prevent its movement during measurement.

This type of scanner is popular in industrial applications, where it is used to measure deviations from the required dimensions, for example, when checking geometry or evaluating profiles on defined surfaces or lines.

A great advantage of contact scanners is their ability to accurately scan reflective and transparent surfaces, which can be a problem for optical scanners.

They are also characterized by high accuracy, which can reach up to 1 micron. On the other hand, they have limitations in scanning speed, which can be slower than other methods, and are prone to the risk of damaging the object's surface. They can also be larger in size and price, making them more expensive to use. The most common examples of contact scanners include coordinate measuring machines and measuring arms, which are often used to measure complex surfaces. [1]

A characteristic feature of destructive scanners is that scanning leads to the destruction of the sample. The main advantage of these scanners is the ability to capture not only the external but also the internal structure of the object. Thanks to this, we can analyze complex shapes and internal cavities, which is the main reason why these scanners are used. Before scanning, the sample is embedded in a material that fills the interior of the object and at the same time provides sufficient contrast to its material. During scanning, the sample is firmly placed on a platform, where very thin layers of material are repeatedly removed by milling, and each milled layer is subsequently scanned. This process continues until the material is completely removed. After scanning, the individual layers are digitally processed and assembled, creating a three-dimensional model of the object. [2]

Non-destructive scanners use a stable platform to hold the object and an arm with an end probe that scans the position coordinates. The arm, which can be robotic or manually operated, records the x, y and z coordinates in space when the probe contacts the object. The result is a point cloud that is used to create a 3D model. These scanners, known as CMM (Coordinate Measuring Machines), are widely used in industry, especially for checking the accuracy of manufactured components. Due to the nature of the materials and the scanning method, there is no deformation or damage to the object, which allows for measurement accuracy in the micrometer range.

Non-contact 3D scanners, as the name suggests, allow for remote measurement, which is the main advantage of this type of scanner, which is currently the most widespread on the market. Compared to traditional touch scanners, they are faster, more efficiently scan objects with complex shapes, and are ideal for comprehensive analysis of measured parts. However, non-contact scanners have certain limitations when scanning certain surfaces or capturing fine details on an object. [3,4]

Currently, the following non-contact scanners are proposed to be used [5-8]:

- Laser 3D scanners – A laser scanner projects one or more laser lines onto the surface of the scanned object and then monitors their reflection using a camera.
- Scanners using structured light – scanners work on the principle of triangulation, but instead of a laser, they use a projector that projects different light patterns onto the scanned object.
- Scanners using photogrammetry – the approach consists of taking a series of photographs of the object from different angles using a digital camera. Specialized software then analyzes the images, identifies points common to different photographs, and calculates the remaining surface points using passive triangulation.
- Ultrasound scanners – work on the principle of non-contact scanning of objects using a probe that generates sound waves with a frequency above 20 kHz.
- X-ray scanners – are used to obtain detailed information about the internal structure of an object using X-rays (RTG). The radiation intensity of these devices is higher than that of conventional X-rays in healthcare.

In recent years, 3D scanning in industrial manufacturing has evolved from a quality control tool at the end of the manufacturing process to a tool that has a major impact on all phases of design and manufacturing. This progress has been made possible by technical innovations that have improved the accuracy, portability, and user-friendliness of these devices.

3D scanners were originally used for final quality control, where they served as a decision point to confirm that parts meet specifications. However, today's technologies allow them to be deployed from the very beginning of the process, where they are used to accurately collect data during the design process. This data is then used in generative design, which contributes to the creation of optimized products and reduces the number of adjustments during production. This approach also allows the introduction of Closed-Loop Systems, where data is continuously analyzed and used to improve the quality and efficiency of manufacturing processes. [9]

One of the current trends in the field of 3D scanning is its use in combination with machine learning for surface inspection and defect detection. Originally used primarily in industries such as the automotive industry, this technology is now also being applied in the construction industry, where 3D scanning is combined with machine learning algorithms to automate the detection of surface defects on buildings.

The goal of this innovation is to streamline inspection processes and reduce the time needed to assess building maintenance. The technology not only allows for the detection of defects such as cracks, irregularities or corrosion damage, but also categorizes their severity and provides data for further decision-making. 3D scanning is used to create a digital model of the building, which is then analyzed by machine learning. This approach allows the detection of even very fine details that could be overlooked during manual inspection. [9, 10]

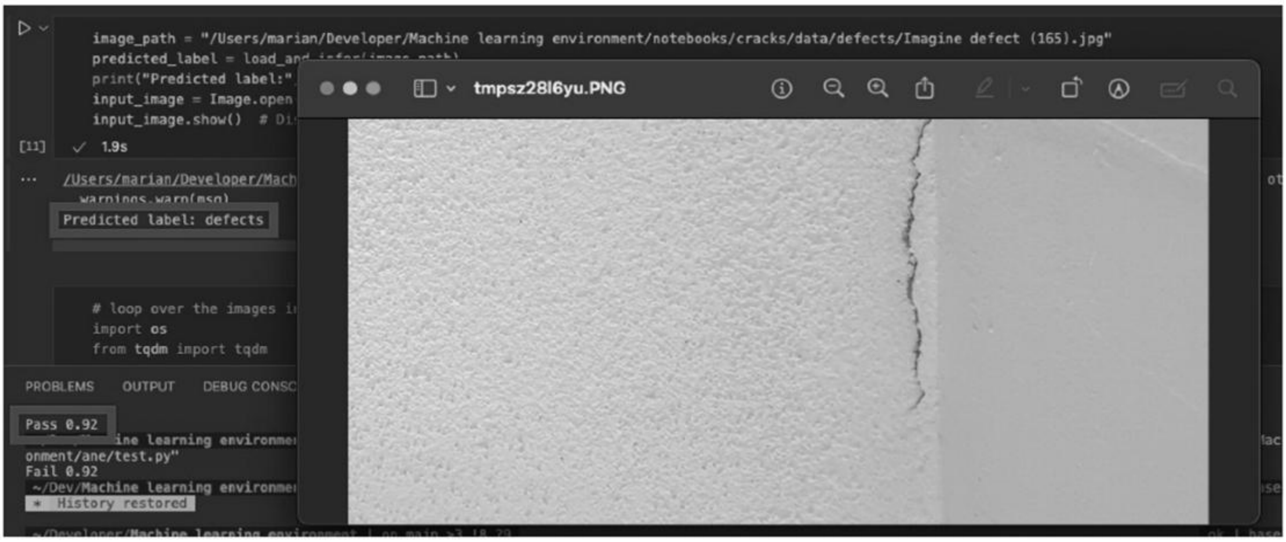

Fig. 1 *Demonstration of defect analysis using machine learning* [10]

Advanced software features play a crucial role in integrating scanned data into designers' workflows. Improved data processing enables faster and more efficient integration of scanned data into CAD software or simulation tools. This advancement not only saves time, but also encourages creativity and allows designers to refine their designs.

In addition, 3D scanning facilitates the transition to Model-Based Definition, where manufacturing and geometric dimensioning and tolerance (GD&T) information is directly integrated into 3D CAD models. This eliminates ambiguity and improves communication between quality control teams and designers.

The portability of 3D scanning technologies is fundamentally changing the design process, especially in industries that deal with large and non-relocatable parts. A key feature of portable scanners is their ability to operate in a variety of environments, with ease of installation, battery life, and wireless connectivity playing important roles.

In industries such as automotive, aerospace, heavy equipment manufacturing, and wind turbines, it is often impossible to move large parts into controlled conditions. Portable scanners allow for accurate scanning in the field, removing the constraints of where the part is located and speeding up the entire design and manufacturing process. The portability of scanners not only increases their flexibility, but also allows them to capture accurate data directly at the manufacturing or production site, which is a major step forward in the field of engineering. With their ease of use and versatility, portable 3D scanners are becoming a key tool for innovation and efficiency in manufacturing.

Automation plays a key role in the OEM (original equipment manufacturer) industry due to limited workforce availability, a shortage of experts, and the need to ensure consistent performance. Quality control processes that use 3D scanning must therefore adapt to these requirements. Automated 3D scanners provide high flexibility and efficiency in quality control and are increasingly integrated with collaborative robots (cobots), which accelerates the digital transformation in manufacturing.

Another significant benefit is the use of digital twins, which allow for real-time monitoring and simulation of manufacturing processes. This technology supports decision-making based on accurate data, contributing to greater efficiency and optimization of manufacturing processes. [10]

The authors have previously addressed this topic in other publications, and this issue will also be a benefit for further research work in our article. [11-13]

2 Measuring the efficiency of tire removal on a conveyor belt

As part of the project, a problem occurred when detecting tire damage on a roller conveyor. The customer provided feedback that the greatest impact on the accuracy of the evaluation was the disturbing effect of direct sunlight, which affected the scanning performance of the 3D scanner.

Fig. 2 shows a view of the newly designed measuring box in a completely assembled form on a roller conveyor. In the box, they were installed on a 3D scanner labeled O3D302 (Fig. 3). This is an advanced industrial sensor using Time-of-Flight (ToF) technology to accurately measure distances and detect objects in three-dimensional space. It works on the principle of transmitting infrared light (850 nm), which is reflected from surfaces and analyzed back by the sensor. Based on the return time of the light, a 3D image is then created.

The 3D scanner was used with the "IFM Vision Assistant" software, which allows not only camera settings, but also visualization of the image captured by the camera. This software contains pre-set applications for various evaluation tasks (Depalletising, Robot Pick & Place, Completeness Monitoring, Object Dimensioning or Level Monitoring) – see Fig. 4 [14]

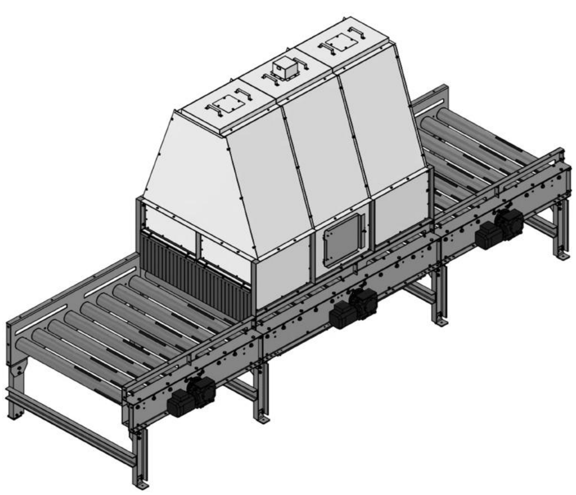

Fig. 2 *Test track assembly – measuring box [author]*

Fig. 3 *Tire rolling resistance at different inflation pressures [4]*

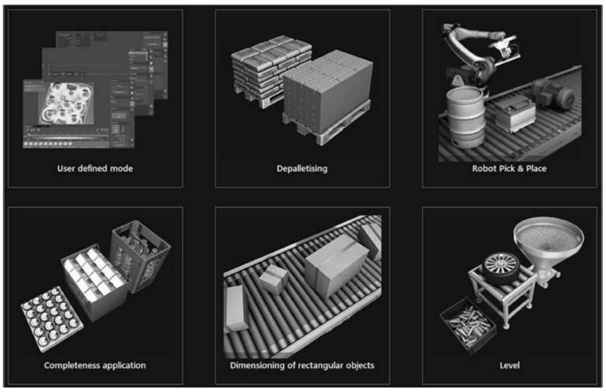

Fig. 4 *Software and 3D scanner applications [15]*

As part of the control testing, the quality of spatial 3D data obtained using a 3D scanner under various simulated conditions was compared. This data is recorded in the form of a so-called point cloud - a three-dimensional structure composed of individual points representing the shape of the scanned object. Various external conditions (problematic) were simulated experimentally, such as solar radiation (especially infrared radiation), rain.

To compare 3D data obtained with and without various environmental conditions, I made a test structure. It is assembled from electrical installation profiles and firmly attached to the conveyor.

Fig. 5 *Test track – tire control measurement [author]*

The values of the basic dimensions of the tires were obtained from the scanner - specifically their diameter, width. These values were then compared between individual test conditions. For clarity and easier evaluation, the results were processed into comparison graphs that show how environmental influences affect the quality and reliability of the measurement. A standard tire of the Nokian Tyres WR D4 215/55 R16 type was chosen for the purposes of the experiment. The aim of this section is to describe its basic geometric properties and create a reference data set, which will subsequently be used for comparison with the values obtained using the 3D scanner. As part of the tire measurement, the diameter and width were measured at various positions around the circumference. The measured values are shown in Tab. 1. Based on these data, the average value and standard deviation for both values were calculated.

Tab. 1 *Measured tire dimensions [author]*

Measurement	Width [mm]	Average [mm]
1	214.0	631.0
2	216.0	630.0
3	214.0	633.0
4	215.0	633.0
5	216.0	631.0
6	215.0	634.0
7	215.0	631.0
8	216.0	631.0
9	216.0	630.0
10	215.0	632.0
11	214.0	634.0
12	215.0	634.0
$\bar{x}$	**215.1**	**632.0**
σ	**0.8**	**1.5**
MAX dimension	**215.9**	**633.5**
MIN dimension	**214.3**	**630.5**

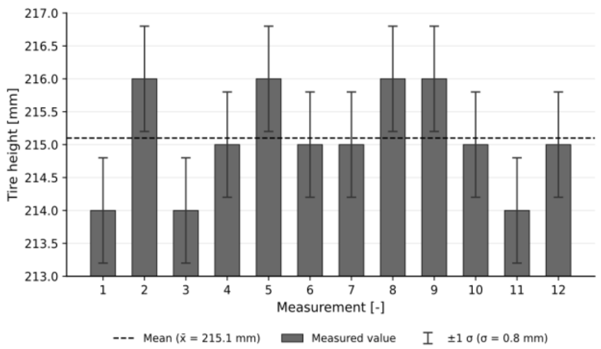

Fig. 6 *Measured values of the control tire height [author]*

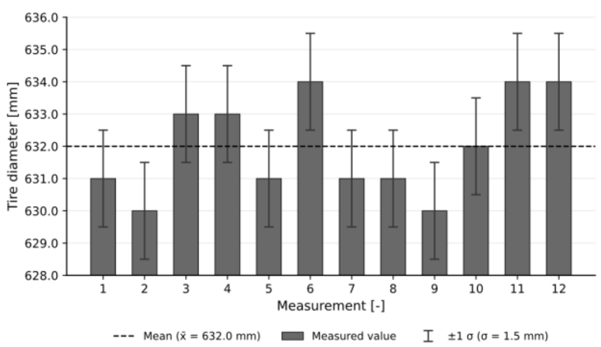

Fig. 7 *Measured values of the control tire diameter [author]*

Based on these values, the actual tire dimensions can be compared with the scan results and the measurement accuracy can be evaluated. The average value (215.1 mm for width and 633.5 mm for diameter) was used to compare the data, while the maximum and minimum values from Table 1 (MAX and MIN dimensions) were used only for visual representation of the range in the graph.

2.1 Description of simulated states

Without artificially simulated conditions – No conditions were artificially simulated in this testing, but real environmental conditions were assessed. In order to make comparisons possible, it is necessary to ensure that testing, with and without measures, takes place with the shortest possible time delay, so that external conditions are as similar as possible.

Rain simulation – Rain can affect transmitted and received infrared radiation in various ways. For example, by absorbing radiation by water, scattering radiation in different directions. A pressure sprayer was used for the simulation for testing without a box and other measures. For the purposes of simulating rain with a test box, a water hose equipped with an adjustable spray head was used, allowing regulation of the intensity and nature of the water stream.

Simulation of solar radiation – Solar radiation consists of 3 types of radiation:

- Ultraviolet (UV) – wavelength below 380 nm, proportion 0 to 4%,
- Visible – wavelength 380 to 780 nm, proportion 21 to 46%,
- Infrared (IR) – wavelength over 780 nm, proportion 50 to 79%.

Due to the high proportion of infrared radiation with a wavelength above 780 nm, interference with the 3D scanner, which emits infrared radiation with a wavelength of 850 nm, may occur. To simulate this phenomenon, an infrared lamp "Red light panel BrainLight 300 START", which has wavelengths from 660-850 nm, was used. As part of this testing, the lamp will be placed in various positions and angles around the conveyor.

Fig. 8 *Infrared lamp [16]*

2.2 Measurement results – testing without a protective box

2.2.1 Without Artificially Simulated States (WASS)

Fig. 9 and 10 show a clear occurrence of 3D data deviations (in the point cloud). The tire surface is not very consistent here, with significant fluctuations in the color spectrum, which indicate uneven scanning. The uneven tire profile and higher noise levels can be caused by unwanted external influences, such as ambient sunlight, light reflection, etc. It can be noted that the software correctly recognized the tire number (black line along the tire circumference and number in the middle).

There was also a temporary appearance of significant peaks, as can be seen in Fig. 11.

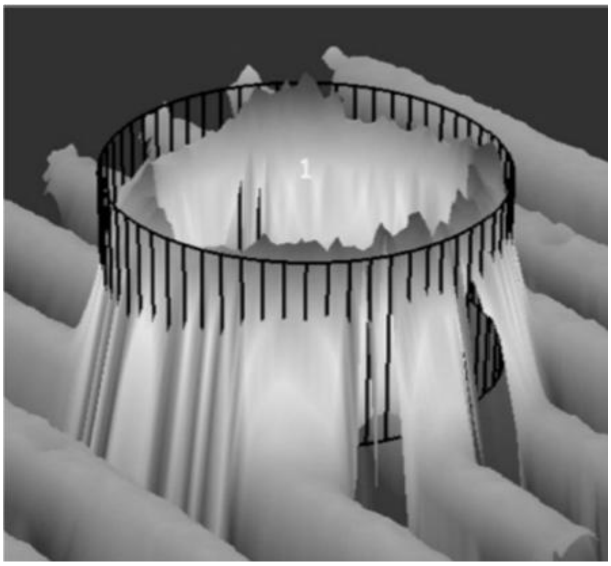

Fig. 9 *WASS – measurement no. 1 [author]*

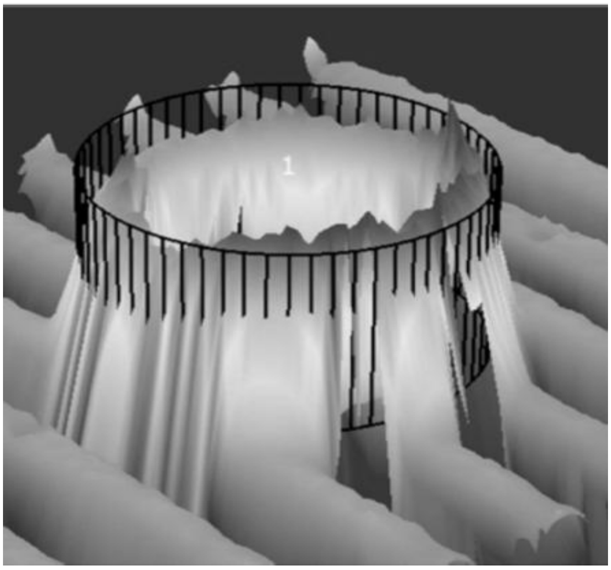

Fig. 10 *WASS – measurement no. 2 [author]*

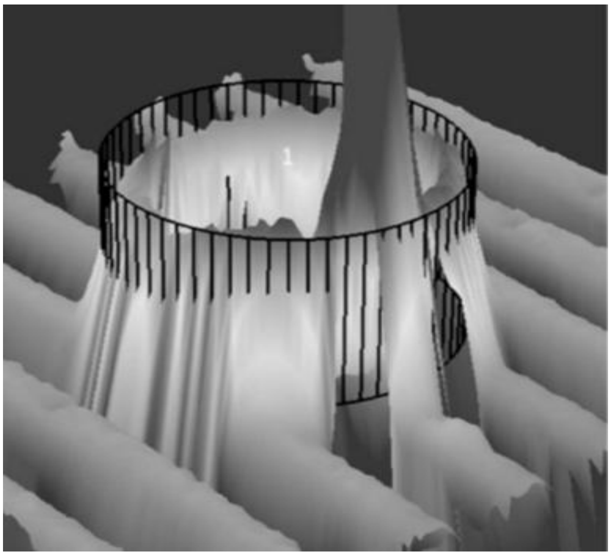

Fig. 11 *WASS – measurement no. 3 [author]*

2.2.2 Simulation of Solar Radiation (SSR)

In Fig. 12 to Fig. 13, more significant deviations in the spatial reconstruction of the tire surface are visible than in the previous case (without artificially simulated states). The tire surface is less consistent here, which is reflected in significant fluctuations in the color spectrum.

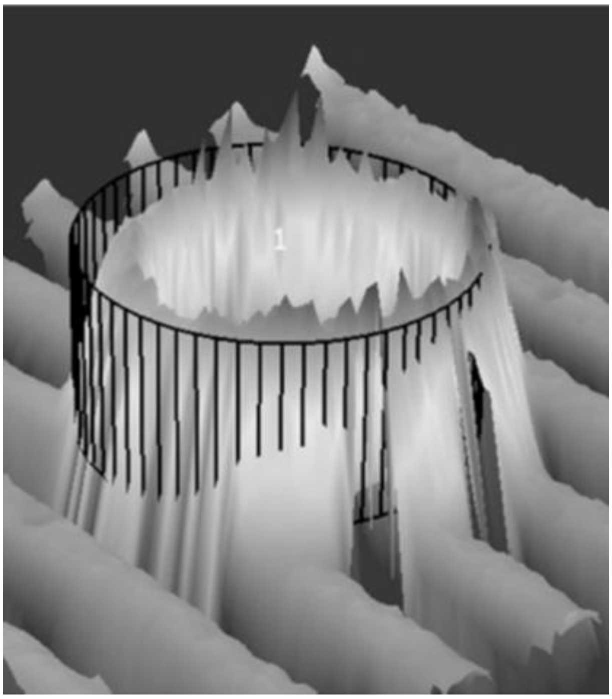

Fig. 12 SSR – measurement no. 1 [author]

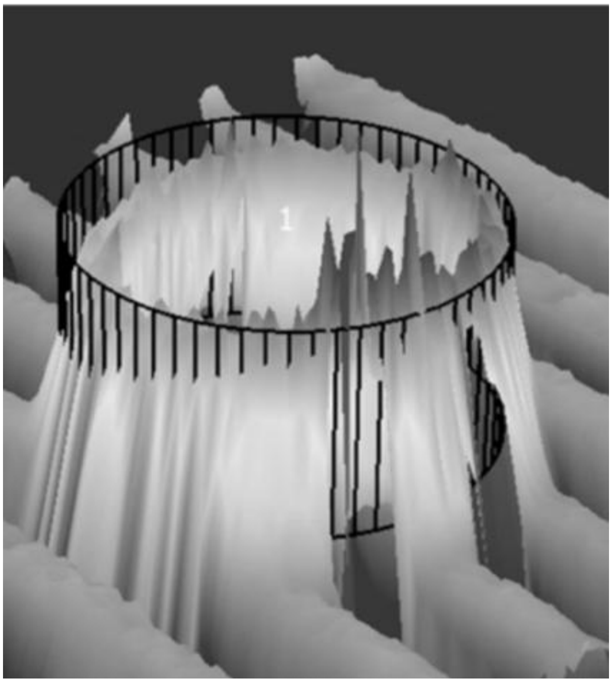

Fig. 13 SSR – measurement no. 2 [author]

Peaking was more frequent with much more pronounced deformation. The software misinterpreted the tire dimensions – see Fig. 14.

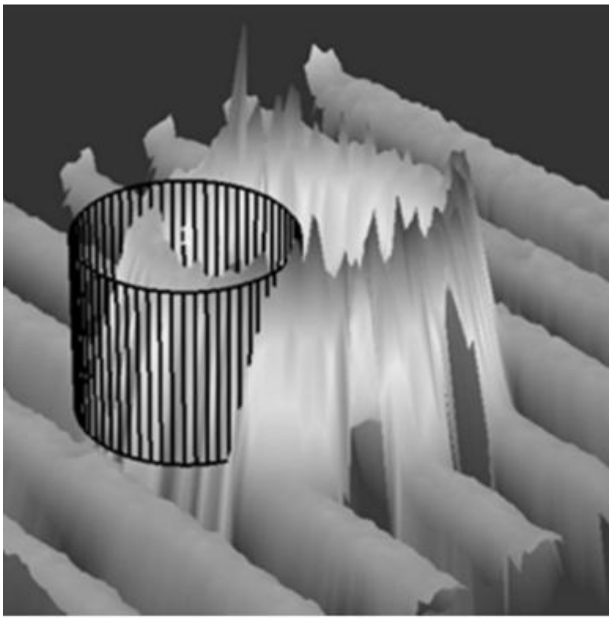

Fig. 14 SSR – measurement no. 5 [author]

2.2.3 Simulation of Rain (SR)

Rain causes significant deviations in the 3D point cloud, which is manifested by increased noise and artifacts. These errors can be caused by unwanted reflections of water on the tire and conveyor surfaces, which affect the correct depth triangulation. The black reference line shows deformations, which indicates that the software has incorrectly interpreted the geometry of the scanned object.

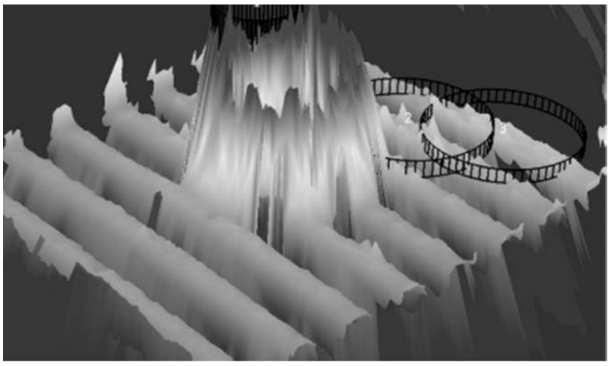

Fig. 15 SR – measurement no. 2 [author]

2.2.4 Wet Tire (WT)

For a wet tire, there are significant fluctuations in the measured values, with extreme peak anomalies visible on the tire surface. These deviations may be caused by uneven scattering and absorption of the laser beam on the wet surface, which distorts the obtained dimensional data (tire height, diameter).

Tab. 2 shows the measured data from the scanner under various conditions without the use of a protective box or cover. When measuring without artificially simulated conditions (BUSS), an average width of 238.8 mm and a diameter of 635.9 mm were recorded. The deviation of the diameter from the reference value was only 2.4 mm, which is a relatively low value. However, due to the higher standard deviation, these results cannot be considered sufficiently accurate. In the case of the width, a more significant overestimation of approximately 23.7 mm was recorded. The standard deviation was 7.9 mm for the width and 13.6 mm for the diameter, which indicates considerable variability, especially in the diameter measurement.

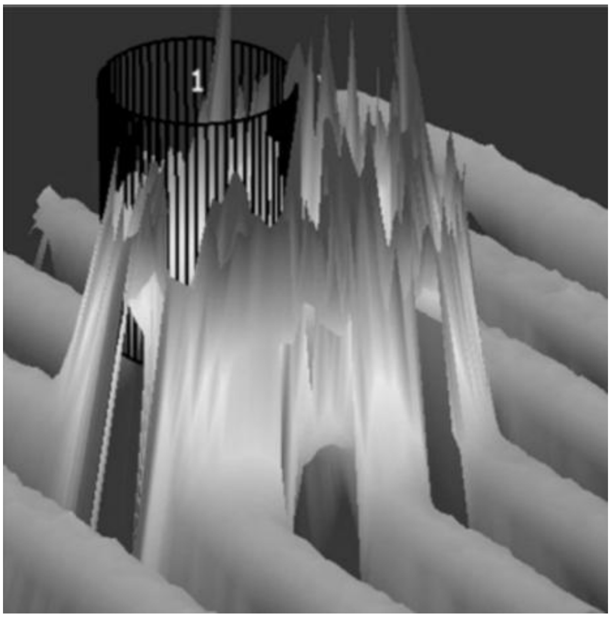

Fig. 16 *WT – measurement no. 1 [author]*

When simulating solar radiation (IR), the width slightly increased to 244.8 mm, while the diameter decreased to 611.2 mm. The deviation of the diameter thus reached a value of 22.3 mm, which indicates a significant deterioration in accuracy. The dispersion of the measured data also increased significantly, the standard deviation of the average increased to 87.8 mm, which confirms the significant instability of the measurement in these conditions.

The rain simulation was not evaluated, because the output data was so distorted that it did not allow a relevant comparison with other conditions. For this reason, the results are not shown in the table.

The worst results were achieved when measuring a wet tire. The average width was 298.3 mm, which is an overestimation of 83.2 mm. The diameter was underestimated to a value of 481.8 mm, i.e. 151.7 mm lower than the reference value. High standard deviations, specifically 30.8 mm for the width and 119.2 mm for the diameter, confirm the significant negative influence of a wet and shiny surface on the accuracy of optical sensing.

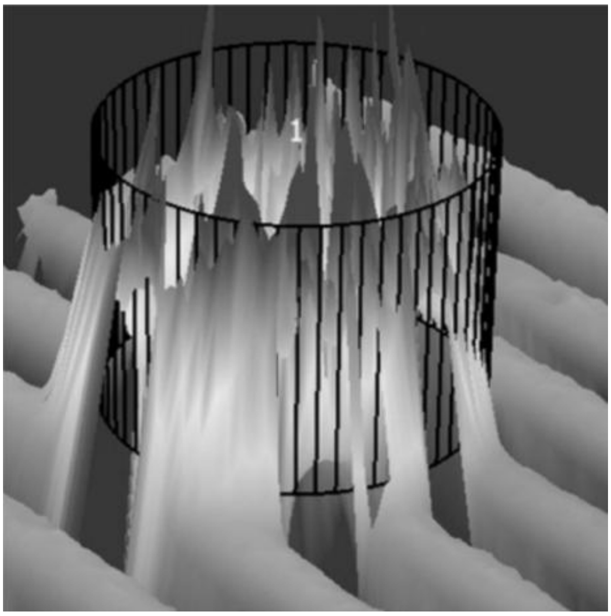

Fig. 17 *WT – measurement no. 2 [author]*

Tab. 2 *Measured tire dimensions [author]*

	WASS		IR		WT	
	Width [mm]	**Diameter [mm]**	**Width [mm]**	**Diameter [mm]**	**Width [mm]**	**Diameter [mm]**
1	246	632	251	629	327	290
2	230	615	246	644	313	337
3	241	626	235	650	258	490
4	230	661	235	670	306	556
5	249	653	244	655	254	449
6	225	637	252	324	307	557
7	231	643	249	635	276	281
8	247	624	236	627	343	624
9	245	630	250	615	333	611
10	235	624	244	635	285	609
11	241	655	247	622	325	430
12	246	631	248	628	253	548
$\bar{x}$	**238.8**	**635.9**	**244.8**	**611.2**	**298.3**	**481.8**
σ	**7.9**	**13.6**	**5.9**	**87.8**	**30.8**	**119.2**
* WASS - Without Artificially Simulated States, SSR - Simulation of Solar Radiation WT – Wet Tire						

The most stable results were achieved when measuring without artificially simulated conditions, while the presence of infrared radiation led to a slight decrease in accuracy. In the case of a wet tire, the greatest data distortion and increase in dispersion occurred, which indicates the fundamental influence of the glossy surface on the scanner's operation.

2.3 Measurement results – testing with a protective box

2.3.1 Without artificially simulated states (WASS)

The tire surface was scanned evenly with minimal noise or artifacts. The black reference line correctly follows the object's contour and the color scale corresponds to consistent elevation data capture. Part of the tire contour is missing from the front of the tire. Most likely due to poor ray reflection.

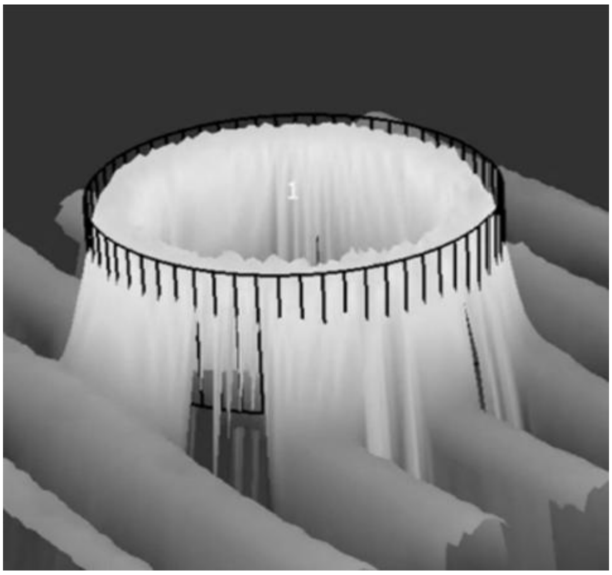

Fig. 18 *WASS – measurement no. 1 [author]*

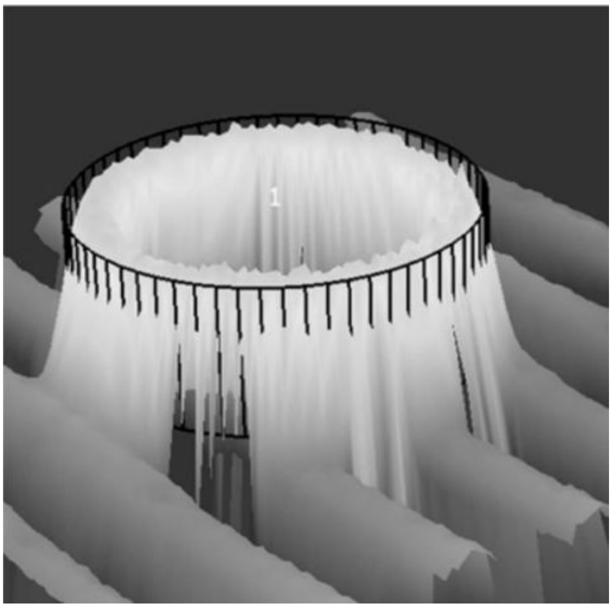

Fig. 19 *WASS – measurement no. 2 [author]*

2.3.2 Simulation of Solar Radiation (SSR)

The influence of infrared radiation is reflected in the images by small local fluctuations in the point cloud, especially in the area between the rollers. These deviations can be caused by holes in the side of the conveyor through which the radiation passes.

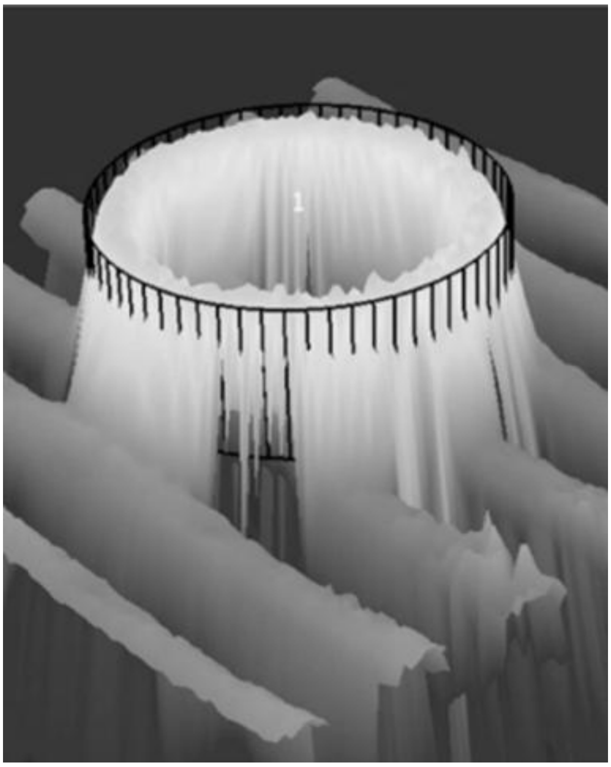

Fig. 20 *SSR – measurement no. 1 [author]*

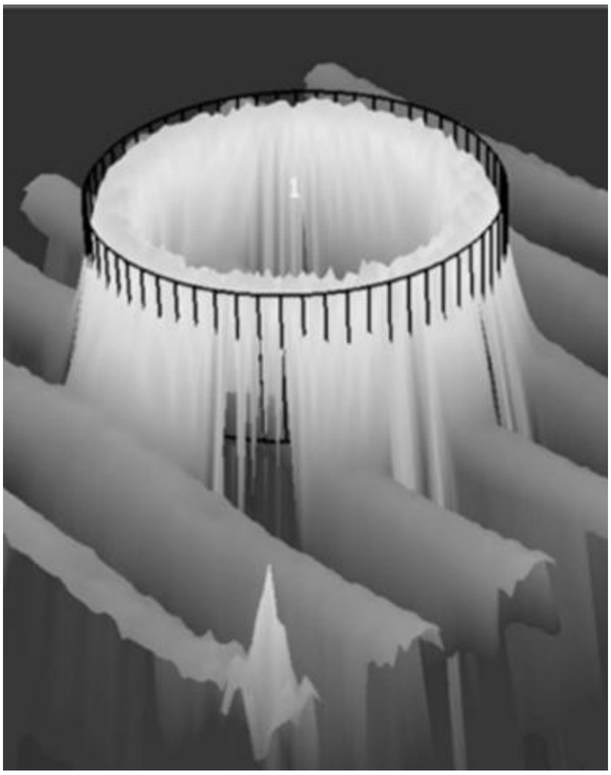

Fig. 21 *SSR – measurement no. 2 [author]*

2.3.3 Simulation of Rain (SR)

In Fig. 22 and 23, a significant level of interference is evident in the form of sharp peaks extending above and beyond the tire area, caused by simulated rain.

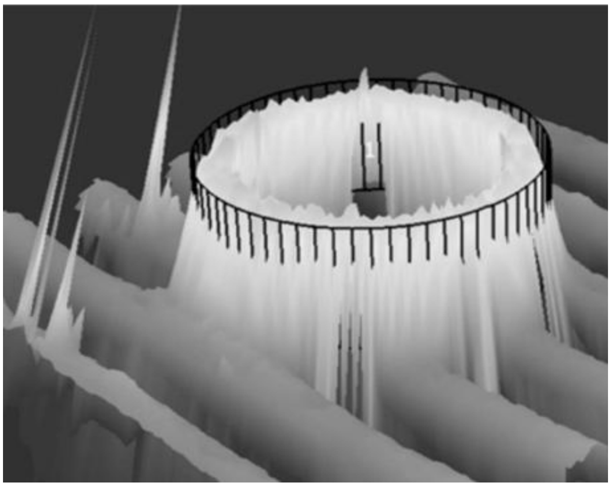

Fig. 22 SR – measurement no. 1 [author]

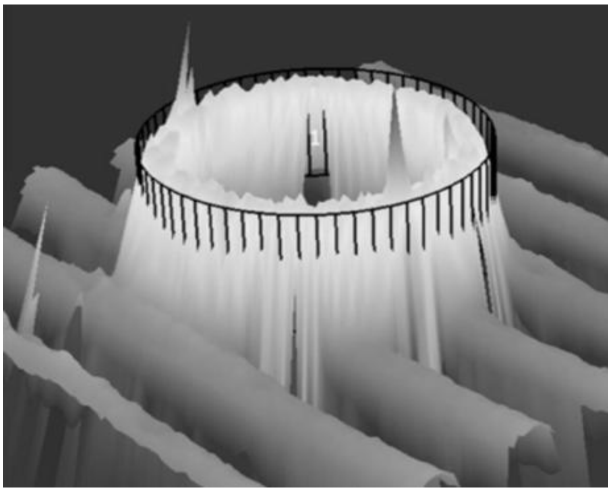

Fig. 23 SR – measurement no. 2 [author]

2.3.4 Wet Tire (WT)

The presence of water on the tire surface causes some level of pitch noise, but overall object recognition is more stable than without using the box.

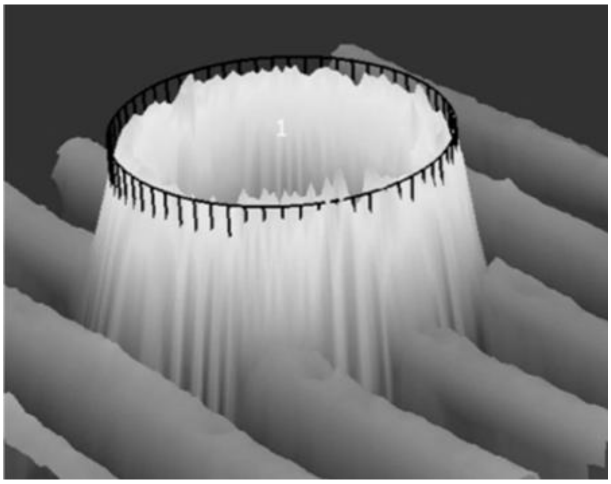

Fig. 23 WT – measurement no. 1 [author]

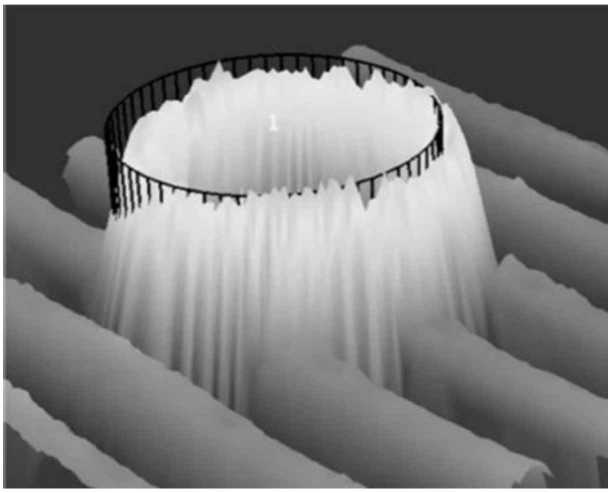

Fig. 24 WT – measurement no. 2 [author]

Tab. 3 Measured tire dimensions [author]

	WASS		IR		SR		WT	
	Width [mm]	Diameter [mm]	Width [mm]	Diameter [mm]	Width [mm]	Diameter [mm]	Width [mm]	Diameter [mm]
1	221	620	230	625	231	626	233	626
2	220	619	226	623	234	631	231	625
3	223	622	230	622	236	631	232	627
4	221	621	228	624	236	627	229	626
5	221	620	235	623	239	627	230	627
6	223	621	230	621	231	630	231	625
7	221	620	224	624	233	626	229	626
8	227	621	226	623	231	624	230	626
9	219	622	228	622	234	630	231	625
10	222	619	242	623	231	630	230	627
11	225	622	227	621	236	627	232	624
12	220	621	243	626	233	625	230	626
$\bar{x}$	**221.9**	**620.7**	**230.8**	**623.1**	**233.8**	**627.8**	**230.7**	**625.8**
σ	**2.2**	**1.0**	**5.9**	**1.4**	**2.5**	**2.3**	**1.2**	**0.9**
* WASS - Without Artificially Simulated States, SSR - Simulation of Solar Radiation, SR – Simulation of Rain, WT – Wet Tire								

3 Discussion and Conclusion

As part of the control testing of the newly designed protective box, several scanning variants were performed, which differed in the degree of coverage and the presence of disturbing external factors. The measurement results showed how significantly the quality of the output data from the 3D camera can fluctuate depending on the ambient conditions and the technical solution of the workplace.

When shooting without any masking, the results were the least satisfactory. The camera was exposed to ambient light and light reflections, which caused extensive artifacts, peaking and significant deformation of the 3D point cloud data. The measurements showed high variability and significant deviations, and the results were very distorted. After installing the box, the interference was partially reduced, the tire contours were better defined and the background noise was reduced. However, the best results were achieved only in the configuration with complete coverage from above and below (bottom masking), where the images were the cleanest, with a minimum of false points outside the tire area. The use of masking significantly improved the stability of the measurements and minimized deviations.

When simulating sunlight from the top of the conveyor without a cover, there was significant interference and deformation of the point cloud. Adding the box significantly improved the quality, the scan was more stable. Slight noise still appeared on the edge of the conveyor, where the hole for the position sensors is located. After adding the bottom cover, the interference still persisted. A possible solution is to cover the hole on the side of the conveyor in places where the position sensor is not located.

When simulating sunlight from the bottom of the conveyor without a cover, it caused less interference than from above, but distortion was still evident in the tire area. Using the box significantly reduced the interference, and in combination with the bottom cover, the quality of the point cloud significantly improved and did not show noticeable deviations.

When simulating rain, whether with or without a cover, there was a significant increase in artifacts caused by water drops and reflections. Scanning without covering was the most prone to errors – deformations of the reference line and disturbing peaks occurred throughout the field. Using the box managed to partially reduce interference from the surrounding environment, but the noise level was still noticeably higher than in the experiment without rain. Here too, it was clear that proper covering helps, however, the presence of water as a reflective surface remains a problem and significantly affects the accuracy of the measurement.

In order to eliminate the negative impact of water flowing into the scanning area, it would be appropriate to consider the structural modification of the box, especially its upper part. The roof should be modified so that it drains water outside the inner part of the box.

When scanning a wet tire without covering, the point cloud was significantly disturbed and strongly distorted, the recognition of the tire shape was inaccurate, often even outside the real position. Using the box helped to partially stabilize the situation, the scan already captured the basic contours of the tire, but still with the presence of errors. Adding the lower covering led to a slight improvement, but there were still small interferences.

During testing, it turned out that evaluating a 3D scanner using only volume is not ideal. Therefore, an alternative solution was found in the form of a scanner that can evaluate the number of holes in the point cloud, which allows for more accurate detection of specific problems, such as identifying a tire with a disk, tire damage, or the presence of two tires inside each other. Another advantage of this scanner is a wider angle of view. Thanks to these features, it is possible to design a lower box, which will bring advantages not only in scanning quality (higher resolution), but also in the area of maintenance and access to the device. The structural change of the box will be simple, just reduce the length and height of the folded sheets of the middle part of the box.

We also recommend testing the effectiveness of the matte coating of the inner part of the box, which could help reduce ray reflections and thus limit optical interference. It would also be appropriate to supplement the testing with tests during operation, i.e. with vibrations and during the operation of the conveyor, in order to comprehensively evaluate the influence of these factors on the accuracy of scanning.

When simulating sunlight from the top of the conveyor without a cover, there was significant interference and deformation of the point cloud. Adding the box significantly improved the quality, the scan was more stable. Slight noise still appeared on the edge of the conveyor, where the hole for the position sensors is located. After adding the bottom cover, the interference still persisted. A possible solution is to cover the hole on the side of the conveyor where the position sensor is not located.

Acknowledgement

This article was created with the support of grant UJEP-SGS-2024-48-001-2.

References

[1] MENDŘICKÝ, R., KELLER, P. (2015) 3D skenery pro použití v průmyslu. Automa. *Automa-časopis pro automatizační techniku*, 2015(12), 34-37. ISSN 1210-9592.

[2] ČEPOVÁ, L., PETŘKOVSKÁ, L. Legislativa ve strojírenské metrologii a přesné měření 3D ploch. *Studijní opora. Ostrava*: Vysoká škola báňská - Technická univerzita Ostrava, 2011. ISBN 978-80-248-2514-4.

[3] BELLOCCHIO, F. 3D surface reconstruction: multi-scale hierarchical approaches. New York: *Springer*, 2013. ISBN 14-614-5631-2.

[4] EBRAHIM, M. A. B. 3D Laser Scanners Techniques Overview [online]. 4. Raipur: *International Journal of Science and Research*, 2015 [cit.2025-05-11]. ISSN 2319 – 7064. From: https://www.researchgate.net/publicatio/282753883_3D_Laser_Scanners'_Techni

[5] RAJA, V., FERNANDES, K. J.. Reverse engineering: an industrial perspective. *London: Springer. Series in advanced manufacturing (Springer)*, 2008. ISBN 978-1-84628-856-2.

[6] SCHONBERGER, J. L.; FRAHM, J. M. Structure-from-motion revisited. In: *Proceedings of the IEEE conference on computer vision and pattern recognition*. 2016. p. 4104-4113.

[7] Technologie skenování ve 3D. SPSKS [online]. 2007 [cit. 2025-05-11]. From: https://docplayer.cz/17600850-Spsks-cz-technologie-skenovani-ve-3dzpracovano-v-ramci-projektu-cz-1-07-3-2-10-04-0024-financovaneho-z-fondueu.html#show_full_text

[8] Industrial CT. In: HAMAMATSU K. [online]. Hamamatsu Photonics. [cit. 2025-05-11]. From: http://www.hamamatsu.com/us/en/community/xndt/appindustrial/industrial_ct.html

[9] Design Engineering. 3D Scanning Trends in Engineering. [online] [cit. 2025-05-11] From: https://www.design-engineering.com/features/3d-scanningtrends-engineering/

[10] MARINIUC, A. M.; COJOCARU, D.; ABAGIU, M. M. Building Surface Defect Detection Using Machine Learning and 3D Scanning Techniques in the Construction Domain. *Buildings 2024*, 14, 669. From: https://doi.org/10.3390/buildings14030669

[11] ZHAO H. Design of a Photoelectric Measuring Robot for Straightness of Deep/Blind Hole with Automatic Centering Function. *Manufacturing Technology*. 2023;23(5):739-749. doi: 10.21062/mft.2023.098.

[12] CEDZO M, HOLUBJÁK J, CZÁNOVÁ T, TIMKO P, KOZOVÝ P, DRBÚL M. Analysis of the Substitutability of Conventional Technologies in the Design of a Clamping Vise for Measurement Using an Optical Measuring System. *Manufacturing Technology*. 2023;23(2):136-142. doi: 10.21062/mft.2023.028.

[13] ZHANG H, CHEN H, HU L. Research on Grinding Parameters of Parts with Same Clamping Mode and Different Sizes. *Manufacturing Technology*. 2022;22(3):377-383. doi: 10.21062/mft.2022.035.

[14] IFM Electronic gmbh [online]. [cit. 2025-05-11]. From: https://www.ifm.com/de/en/product/O3D302

[15] IFM. O3D302 Manual. [online]. [cit. 2025-05-11]. From: https://media.ifm.com/CIP/mediadelivery/asset/db84c9dc7211104091441e533b1d5b96/7391232_EN.pdf?contentdisposition=inline

[16] Natur-life. [online]. [cit. 2025-05-11]. Dostupné z: https://naturlife. cz/product/blight-red-light-panel-brainlight-300-start-no-flicker